scientific reports

Check for updates

OPEN

Optogenetic regulation of chloride ions in reactive astrocytes may mitigate Parkinson's disease pathology

Eun Jung Lee[1], Hyung Ho Yoon[2] & Sang Ryong Jeon[2]✉

Recent investigations underscore the pivotal role of reactive astrocytes in the pathogenesis of Parkinson's disease (PD). As PD advances, reactive astrocytes lose their ability to degrade α-Synuclein (α-Syn) aggregates while concurrently increasing *r*-aminobutyric acid (GABA) secretion, which heightens inhibition of DA neurons and worsens the disease. This study explored optogenetic manipulation of reactive astrocytes as a therapeutic strategy. Halorhodopsin (NpHR), a chloride pump, was expressed in reactive astrocytes within the substantia nigra pars compacta (SNpc) of an A53T α-Syn overexpression PD rat model. Optogenetic stimulation of NpHR led to a 72.6% reduction in GABA level ($p = 0.0486$) and a 67.5% decrease in α-Syn aggregates ($p < 0.0001$) within the SNpc. Furthermore, contralateral forelimb akinesia was significantly improved by 81.4 ± 7.2% (71.6–90.9%) post-illumination in the NpHR group compared with the pre-illumination state ($p = 0.0002$). These results suggest that the optogenetic modulation of reactive astrocytes can alleviate astrocytic aberrant tonic inhibition of DA neurons, resulting in the revitalization of DA neurons and enhancing the degradation of α-Syn aggregates. This mechanism may ultimately ameliorate parkinsonian motor symptoms, suggesting a promising novel therapeutic avenue for PD.

Keywords Alpha-synuclein, GABA, Halorhodopsin, Optogenetics, Parkinson's disease, Reactive astrocyte

Parkinson's disease (PD) is the second most prevalent neurodegenerative disease and characterized by the progressive accumulation of misfolded α-synuclein (α-Syn). This protein aggregates sequentially into oligomers and protofibrils, culminating in the formation of Lewy bodies, which are pathognomonic intraneural inclusions[1–4]. These α-Syn aggregates are toxic, compromising the integrity of various microorganelles, precipitating synaptic dysfunction and, ultimately leading to progressive neuronal loss[5]. Dopamine (DA)-producing neurons are notably susceptible to α-Syn pathologies, and neuronal degeneration underlies the cardinal motor symptoms of PD, including resting tremor, bradykinesia, and rigidity[6]. Deep brain stimulation targeting the subthalamic nucleus or globus pallidus is a well-established therapeutic modality that significantly ameliorates parkinsonian symptoms in patients with advanced PD by restoring signaling within disrupted cortico-basal ganglia-thalamocortical circuits[7–9]. However, the literature remains inconclusive regarding the potential disease-modifying properties of DBS beyond mere symptom relief[10,11]. Instead, therapeutic interventions that directly target α-Syn aggregates, which are considered fundamental to the pathogenesis of PD, to antagonize their formation or increase their degradation have been embraced as the main disease-modifying strategies[5,6]. Recently, however, there has been a pivotal shift in focus toward the role of reactive astrocytes in initiating and promoting degeneration in PD, as these cells were found to increase *r*-aminobutyric acid (GABA) synthesis and aberrantly release tonic GABA, leading to elevated suppression of DA neurons[12–16]. An intriguing discovery was the existence of dormant DA neurons, which, although functionally inactive and negative for tyrosine hydroxylase (TH), remain viable and continue to express DOPA decarboxylase (DDC)[16]. Given that GABA synthesis in astrocytes is facilitated by monoamine oxidase B (MAO-B), the authors of previous study administered MAO-B inhibitors such as selegiline and safinamide to animal models of PD induced by 1-methyl-4-phenyl-1,2,3,6-tetrahydropyridine and 6-hydroxydopamine. These inhibitors led to a marked decrease in the GABA intensity within reactive astrocytes, the correction of the $GABA_A$ receptor-mediated excessive tonic GABA current in the DA neurons of the substantia nigra pars compacta (SNpc), and an increase in TH expression

[1]Department of Neurosurgery, Seoul National University Hospital, Seoul National University College of Medicine, Seoul, Republic of Korea. [2]Department of Neurological Surgery, Asan Medical Center, University of Ulsan College of Medicine, Seoul, Republic of Korea. ✉email: srjeon190@gmail.com

in TH-/DDC + DA neurons. This restoration of TH expression presents a compelling possibility for reactivating quiescent DA neurons, representing a novel avenue for disease-modifying treatment through the modulation of reactive astrocyte activity. However, MAO-B is widely expressed in both astrocytes and serotonergic neurons throughout the brain—including the striatum, hippocampus, midbrain, cerebral cortex, cerebellum, and white matter—limiting the specificity of MAO-B inhibitors for the primary regions of PD pathology and potentially resulting in various side effects[17]. Therefore, in this study, an optogenetic approach was employed to more precisely modulate the functions of reactive astrocytes in the SNpc. Given that the resting membrane potential of reactive astrocytes is often depolarized (less negative) because of abnormalities in K-channel expression, causing them to be in a hyperexcitable state,[18–20] we transduced halorhodopsin (NpHR) into reactive astrocytes in the SNpc of an A53T α-Syn overexpressing PD rat model. We hypothesized that NpHR stimulation would reduce aberrant tonic GABA secretion from reactive astrocytes and alleviate parkinsonian symptoms.

Results

Impact of NpHR stimulation of reactive astrocytes in the substantia nigra on mitigating parkinsonism

All animals that received AAV_2-CMV-A53T-*SNCA*-EGFP exhibited contralateral forelimb akinesia 3 weeks after virus injection. In the stepping test performed before optical illumination, the adjusting steps of the contralateral forelimb significantly decreased to 16.5 ± 6.6% (9.1–26.8%) and 17.8 ± 3.9% (12.9–24.6%) of those of the ipsilateral forelimb in the NpHR ($p = 0.0002$) and control groups ($p = 0.0002$), respectively. One hour after optical illumination at 5 weeks after virus injection, the number of adjusting steps of the contralateral forelimb significantly improved, increasing to 89.2 ± 11.3% (65.6–100%) of those of the ipsilateral forelimb in the NpHR group ($p = 0.0002$), an improvement of 81.4 ± 7.2% (71.6–90.9%) compared with the pre-illumination state. In contrast, in the control group receiving PBS instead of AAV_{DJ}-GFAP-*NpHR*-mCherry, contralateral forelimb akinesia deteriorated after illumination, with the number of adjusting steps decreasing to 8.5 ± 3.3% (3.1–13.2%) of the ipsilateral forelimb, a decrease of 49.5 ± 23.2% (9.3–85.1%) ($p = 0.0003$) compared with the pre-illumination state (Fig. 1).

Characteristics of pathological α-Syn transfection and NpHR transduction in the SNpc

Pathological human α-Syn was expressed in both reactive astrocytes and DA neurons. However, regions strongly positive for GFAP and TH tended to exhibit spatial distinctions from α-Syn-positive areas, with GFAP and TH signals diminishing in regions characterized by pronounced α-Syn aggregates (Figs. 2 and 3). In the control group, approximately 14.2 ± 9.3% (3.1–34.0%) of the GFAP-positive areas exhibited co-localization with α-Syn aggregates, whereas approximately 37.7 ± 16.1% (9.7–74.1%) of the TH-positive areas exhibited α-Syn accumulation in the SNpc. NpHR was transduced in 30.1 ± 19.5% (0.9–68.2%) of the astrocytes in the SNpc of the NpHR group; however, it was also transduced in 30.3 ± 11.6% (11.1–49.6%) of the TH-positive neurons. The α-Syn aggregates displayed a mutually exclusive distribution pattern with NpHR, showing reduced accumulation in regions where NpHR was expressed, with the colocalization area accounting for only 13.6 ± 11.0% (0.04–38.0%) of the NpHR-positive area.

NpHR stimulation of reactive astrocytes reduced the amount of α-Syn in A53T-α-Syn overexpression PD model

Compared with that in the control group, the quantity of α-Syn aggregates in the SNpc, both in total and on average per aggregate, significantly decreased by 67.5% ($p < 0.0001$) and 69.8% ($p < 0.0001$), respectively, in the NpHR group (Fig. 2).

Effect of NpHR stimulation of reactive astrocytes on GABA

Intriguingly, there was a significant increase in astrocyte density in the NpHR group ($p = 0.0052$), and the total area of GFAP-positive regions tended to increase in the NpHR group compared with the control group ($p = 0.0674$) (Fig. 3A and B). However, the percentage of astrocytes that overlapped with α-Syn aggregates was

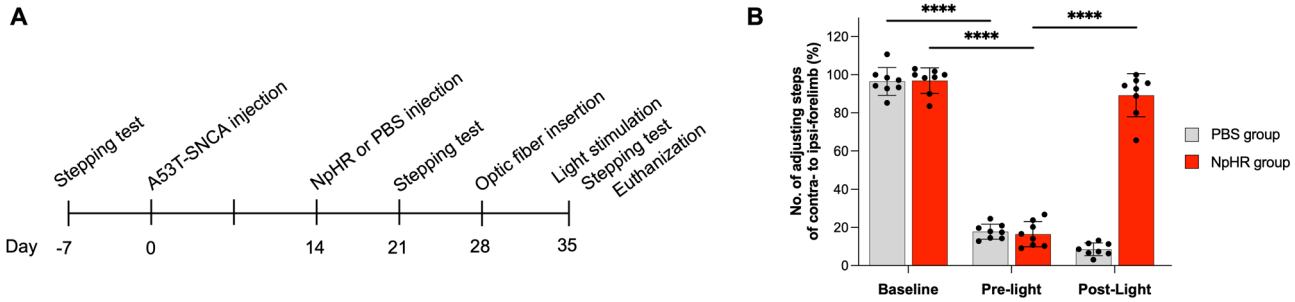

Fig. 1. (A) Timelines of the experiment. (B) Comparisons of contralateral forelimb akinesia in the experimental (NpHR) and control (PBS) groups, as assessed by the percentage of adjusted step numbers of the contralateral forelimb to the ipsilateral forelimb. The leftmost bars represent the baseline values before the onset of parkinsonian symptoms; the middle and rightmost bars represent 35 days after A53T-SNCA injection, pre-illumination and post-illumination, respectively.

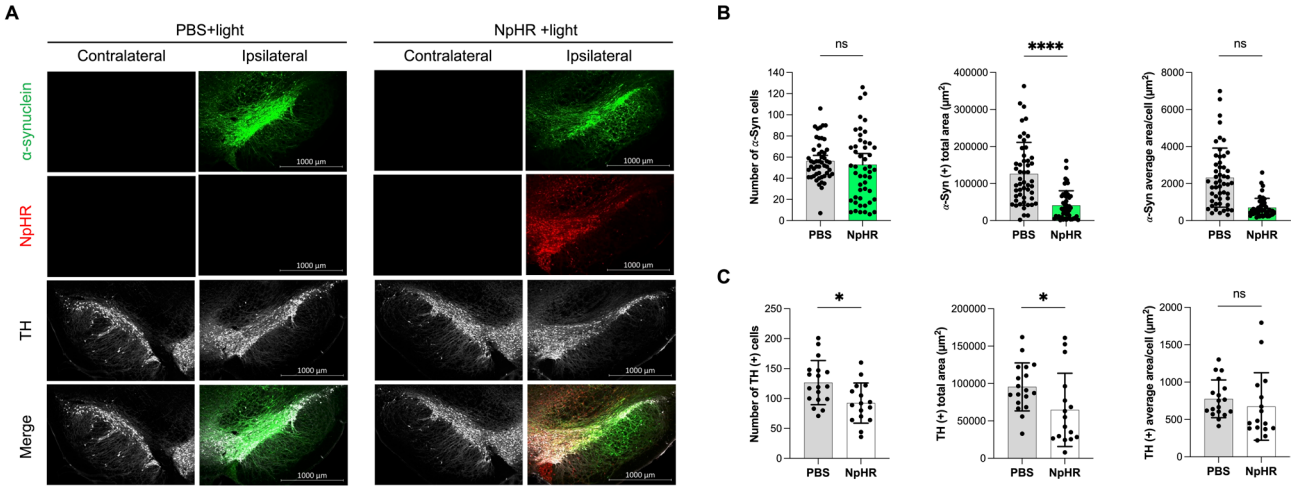

Fig. 2. (A) Distinct spatial distribution patterns are evident in the expression of NpHR, exhibiting mutual exclusivity from α-Syn aggregates. Remarkably, regions displaying NpHR expression show a notable decrease in α-Syn accumulation. Furthermore, the spatial distribution of TH expression is distinct from that of α-Syn signals, with TH expression diminishing in regions where α-Syn aggregates are dense. (A and B) Compared with the control group, the NpHR group demonstrated a significant reduction in both the size of α-Syn aggregates and the overall accumulation of α-Syn in the SNpc, suggesting a notable mitigating effect of NpHR stimulation in reactive astrocytes on the clearance of α-Syn aggregates. (A and C) NpHR expression is detected in approximately 30% of TH-positive cells, as well as reactive astrocytes, resulting in a reduction in both the number and total area of TH-positive cells in the NpHR group compared with those in the control group. However, the decrease in α-Syn aggregates in the NpHR group corresponded to a reduction in TH-positive cells colocalizing with α-Syn. Notably, there was no difference in the number of net TH-positive cells without α-Syn aggregates between the NpHR and control groups.

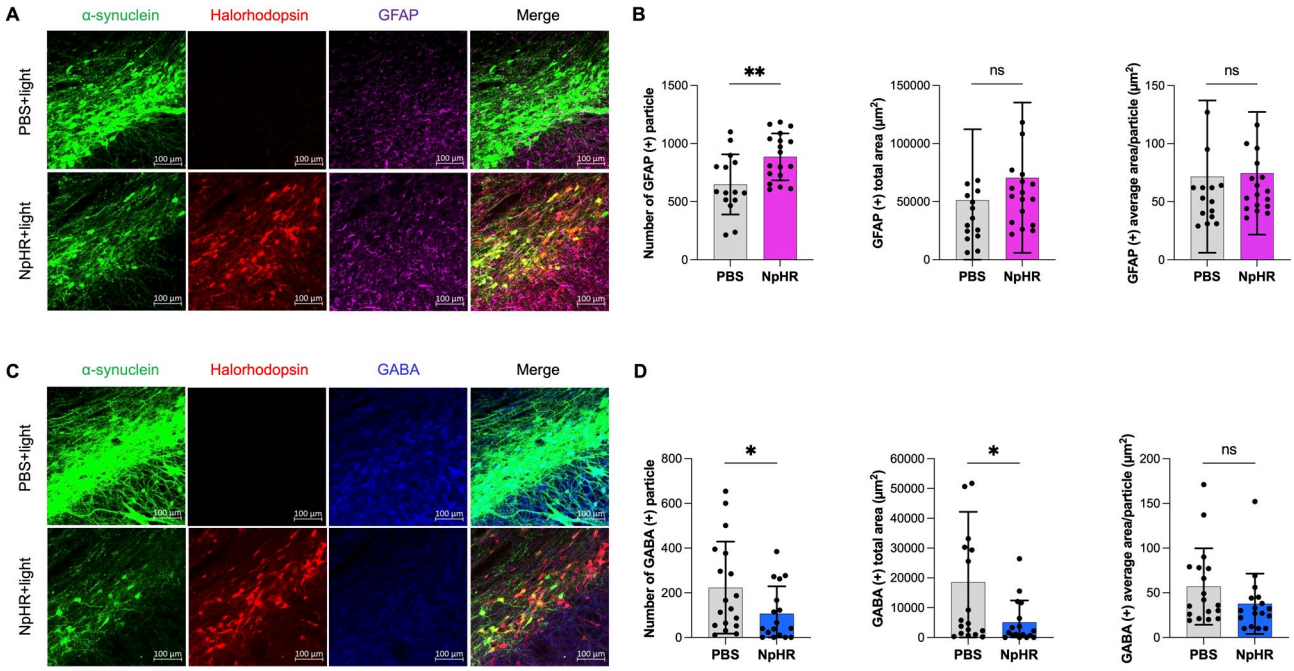

Fig. 3. (A and B) In the NpHR group, the number of GFAP-positive particles in the SNpc was significantly greater than that in the control group, whereas the total area tended to increase. (C and D) GABA levels in the SNpc were significantly lower in the NpHR group than in the control group, corresponding to a significant reduction in α-Syn accumulation in the SNpc.

significantly lower in the NpHR group than in the control group (5.6 ± 4.9% (0.3–16.6%) versus 14.2 ± 9.3% (3.1–34.0%), a decrease of 60.6% ($p = 0.0017$)).

The number of GABA-positive astrocyte and total GABA-positive area were significantly lower in the NpHR group than in the control group by 52.0% ($p = 0.0387$) and 72.6% ($p = 0.0486$), respectively (Fig. 3C and D). The percentage of colocalization area overlapping with the α-Syn aggregates in the GABA-positive area significantly decreased from 31.3 ± 20.4% (1.3–63.2%) in the control group to 9.0 ± 13.7% (0–46.5%) in the NpHR group, a decrease of 71.2% ($p = 0.0002$).

Effects of NpHR stimulation of reactive astrocytes on DA neurons

TH expression was significantly lower in the NpHR group than in the control group, with the TH-positive cell count and total area reduced by 27% ($p = 0.0132$) and 32.2% ($p = 0.0151$), respectively (Fig. 2). However, the percentage of the colocalization area where TH overlapped with the α-Syn aggregates was also significantly lower in the NpHR group than in the control group, at 15.2 ± 10.8% (1.3–39.8%) versus 37.7 ± 16.1% (9.7–74.0%), a decrease of 59.8% ($p < 0.0001$). When the DA neurons with pathological α-Syn aggregates were excluded, the TH-positive DA neuron count and total area were comparable between the NpHR and control groups, with mean values of 78.1 versus 77.7 ($p = 0.7549$) and 56,669 μm^2 versus 58,871 μm^2 ($p = 0.4211$), respectively.

Discussion

The pathological hallmarks of PD are the widespread accumulation of intraneuronal α-Syn aggregates and progressive neuronal cell loss. DA neurons of the SNpc are particularly susceptible to α-Syn pathologies, which lead to the cardinal motor symptoms of PD, such as resting tremor, bradykinesia, and rigidity, manifesting with little as a 30% loss of these neurons[1,12,21]. Previous studies have suggested that damage inflicted on DA neurons by α-Syn is irreversible. However, a recent study revealed that dormant DA neurons, while lacking TH expression, remain viable by continuing to express DDC[16]. The authors demonstrated that these neurons are functionally inhibited by nearby reactive astrocytes and can be rescued. Astrocytes that form a tripartite synapse with neurons express a diverse array of neurotransmitter transporters and ion channels in their membranes, playing crucial roles in maintaining neurotransmitter and ion homeostasis within the tripartite synapse, thereby regulating neural activity[22–25]. Additionally, astrocytes are actively involved in both proinflammatory and anti-inflammatory responses to a variety of central nervous system insults, such as trauma, infection, stroke, brain tumors, and chronic neurodegenerative diseases, with responses varying depending on the nature of the insult[14]. In PD, astrocytes and microglia are pivotal in the clearance of pathological α-Syn. These cells internalize the extracellular α-Syn released by neurons through phagocytosis, pinocytosis, and exosomes and take up α-Syn through tunnelling nanotubules that connect the cytosol of DA neurons and astrocytes[26–28]. Compared with neurons, astrocytes exhibit a superior proteolytic capacity for α-Syn aggregates. This capacity aids in reducing the accumulation of pathological α-Syn within neurons and its propagation throughout the brain, resulting in a neuroprotective effect of reactive astrogliosis in the early stages of the disease[28]. However, as the disease progresses, the continued accumulation of α-Syn in astrocytes eventually overwhelms their lysosomal phagocytic function, promoting the progression of Lewy body pathology and the secretion of inflammatory cytokines by reactive astrocytes, leading to sustained neuronal damage[29–33].

The accumulation of pathological α-Syn in reactive astrocytes induces neuroinflammation, oxidative stress, and disrupted cellular metabolism, leading to elevated polyamine levels, notably putrescine, which serves as a precursor for the synthesis of GABA. Additionally, the expression of MAO-B, a critical enzyme in the GABA synthesis pathway, within astrocytes increases concomitantly with astrogliosis in PD[17]. Consequently, astrocytic GABA synthesis becomes abnormally elevated in PD, leading to its aberrant tonic release into the tripartite synapse, which functionally inhibits DA neurons. Heo et al. reported that the administration of MAO-B inhibitors, such as selegiline and safinamide, resulted in reduced GABA levels and an increased firing rate of DA neurons, leading to the recovery of TH expression and nigrostriatal DA release[16]. These findings indicate that targeting reactive astrocytes could be a promising strategy for disease-modifying treatment. However, previous study has focused primarily on MAO-B and not the reactive astrocytes themselves. Furthermore, while MAO-B is primarily localized in astrocytes, its distribution extends beyond the SNpc to other brain regions, resulting in potential secondary effects of MAO-B inhibitors through the inhibition of GABA synthesis in other regions[17]. Therefore, this study employed an optogenetic technique to more precisely modulate the function of reactive astrocytes in the SNpc. Optogenetics involves the regulation of cellular activity through light stimulation at a specific wavelength via the use of a viral vector to introduce a light-sensitive ion transporter gene, known as microbial opsin, into cells[34–36]. This technique has been utilized primarily in neurons, enabling precise temporal and spatial control of neuronal activity. In contrast, the use of optogenetic approaches in astrocytes has been limited, with most studies focused primarily on the effects of cation channels such as channelrhodopsin under normal physiological conditions[36]. Astrocytes express multiple ion cotransporters and neurotransmitter transporters associated with ion channels, making it challenging to anticipate the effect of modifications of specific ion concentrations within reactive astrocytes in the SNpc in PD models. Nevertheless, considering that reactive astrocytes are typically depolarized by up to 20 mV because of reduced expression of K-channels, resulting in a hyperexcitable state at rest,[18–20] we hypothesized that stimulating NpHR, which induces intracellular chloride ion (Cl^-) influx, in reactive astrocytes would repolarize or hyperpolarize these cells,[37] thereby counteracting aberrant tonic GABA secretion and alleviating parkinsonian symptoms.

This study, pioneering optogenetic modulation of reactive astrocytes in a PD model, presents compelling evidence that one-hour illumination of NpHR expressed in reactive astrocytes within the SNpc effectively reduces GABA levels. Furthermore, a significant reduction in α-Syn aggregates was observed in both DA neurons and reactive astrocytes. Histopathological examination revealed a distinct spatial distribution pattern of NpHR and α-Syn expression, marked by reduced α-Syn deposits in areas with NpHR. In the NpHR group, the

α-Syn aggregates in the SNpc decreased significantly by 68% compared with those in the control group, resulting in an 81.4% improvement in parkinsonian motor symptoms compared with those in the pre-illumination state. These results suggest a potential therapeutic avenue through the modulation of astrocytic activity in PD while concurrently prompting a crucial inquiry: Through which biological process does the elevation of the intracellular Cl^- concentration ($[Cl^-]_i$) within astrocytes contribute to the observed findings?

In PD, reactive astrocytes exhibit aberrant tonic release of GABA, whose synthesis is increased, into the tripartite synapse through the Best1 anion channel[16,20,25,38,39]. The current density of Best1 has been shown to be directly proportional to the membrane potential of astrocytes[38]. Therefore, we speculate that the depolarized membrane potential of reactive astrocytes can be repolarized or hyperpolarized by an increased $[Cl^-]_i$, which, in turn, may reduce the aberrant tonic secretion of GABA via the Best1 channel. Furthermore, the accumulated cytoplasmic GABA in reactive astrocytes can enter the tricarboxylic acid cycle via GABA transaminase and be readily metabolized, further lowering the overall GABA level in the SNpc[39]. This reduction in aberrant tonic GABA secretion by reactive astrocytes is believed to alleviate the functional suppression of DA neurons, thereby restoring neuronal activity. A recent study on Alzheimer's disease and frontotemporal dementia animal models reported that synaptic activation by chronic DBS enhances autophagic–lysosomal degradation, facilitating the clearance of tau oligomers[40]. We speculate that a similar mechanism might underlie our results, where reactivation of the degradation systems in disinhibited DA neurons promotes the removal of α-Syn aggregates and consequently alleviates parkinsonian symptoms. In advanced PD, the diminished capacity for lysosomal acidification in reactive astrocytes is another significant factor that impairs the degradation of α-Syn aggregates[28,31,32]. The $[Cl^-]$ in the astrocytic cytosol is crucial for this process[25,41–43]. Researchers have demonstrated that a low cytosolic $[Cl^-]$ decreases the lysosomal $[Cl^-]$, thereby reducing the activity of the V-ATPase proton pump in the lysosomal membrane[44]. This reduction leads to decreased H^+ influx and increased lysosomal pH. Therefore, it is plausible that an increase in the cytosolic $[Cl^-]$, induced by optogenetic stimulation of NpHR, would restore lysosomal acidification and activate lysosomal hydrolase. We hypothesize that NpHR stimulation would reduce α-Syn aggregates in reactive astrocytes through this mechanism.

Moreover, in the NpHR group, an increase in the overall density of GFAP-positive cells in the SNpc was observed. This finding was unexpected, as it was anticipated that GFAP expression would decrease, corresponding with the reduced GABA and α-Syn deposits in reactive astrocytes. GFAP is a commonly used marker for identifying astrocytes, with elevated expression often indicating increased astrocyte activity[14,45]. Astrocytes undergo reactive astrogliosis, manifesting in two reactive states: A1 and A2[14,46]. The A1 state is neuroinflammatory and releases various complement cascade components, leading to synaptic degeneration and neurotoxicity, whereas the A2 state upregulates neurotrophic factors that support neuronal regeneration and synapse repair[47–49]. Enhanced GFAP expression is observed in both reactive states, making it difficult to ascertain which astrocyte lineage was activated by optogenetic stimulation of NpHR in this study. Further investigation is needed to distinguish between the distinct activation states of reactive astrocytes induced by optogenetic NpHR stimulation.

Our optogenetic technique targeted reactive astrocytes using GFAP as the promoter; however NpHR was also expressed in a subset of DA neurons. Previous research has demonstrated that the activation of NpHR in DA neurons can induce parkinsonism, underscoring the significance of our findings[37]. Specifically, although the total number of TH + DA neurons in the SNpc decreased, NpHR activation in reactive astrocytes resulted in (1) a significant reduction in GABA levels in the SNpc, (2) a decrease in the amount of α-Syn aggregates in DA neurons, and (3) a reduction in the amount of α-Syn aggregates in reactive astrocytes. These changes culminated in substantial alleviation of parkinsonian motor symptoms. These findings suggest that the functional impairment of TH + DA neurons associated with α-Syn accumulation is critical and that a reduction in the amount of α-Syn aggregates is more pivotal for functional recovery rather than a reduction in the absolute number of TH + DA neurons. To validate our findings, future electrophysiological studies are essential to assess changes in the membrane potential, GABA currents via Best1 in reactive astrocytes, and the firing rates of DA neurons in response to in the stimulation of NpHR in reactive astrocytes in a PD model. Fine-tuning the optogenetic parameters and stimulation protocol to establish an optimal level of $[Cl^-]_i$ for restoring Parkinson's pathophysiology without inducing cellular dysfunction will be necessary and warrants additional investigation. Furthermore, a comprehensive exploration of the biochemical mechanisms underlying the reduction in the amount of α-Syn aggregates in both DA neurons and reactive astrocytes is needed.

In summary, our study highlights that modulating the activity of reactive astrocytes, including the $[Cl^-]_i$ levels in these cells, represents a promising strategy for modifying PD, despite the practical limitations of optogenetic techniques. Consequently, more feasible approaches, such as chemogenetic approaches, should be considered for the targeted modulation of reactive astrocytes to treat PD in the future.

Methods and materials

Experimental animals

Sixteen male Wistar rats (Orient Bio, Inc., Seongnam, South Korea), each weighing between 250 and 300 g and aged 8 weeks at the start of the study, were kept in an environment that simulated a 12-hour light and dark cycle, while being allowed free access to food and water. All experimental protocols were reviewed and approved by the Animal Care Committee of the Asan Institute for Life Sciences (approval No. 2020-13-343), Seoul, South Korea. Animal handling, housing, and experimental procedures were performed in accordance with the committee's approved protocol and with relevant institutional guidelines and regulations for the care and use of laboratory animals.

Study design

To investigate the effects of the modulation of reactive astrocytes on the recovery of parkinsonism and elucidate the underlying mechanisms, we transduced NpHR into astrocytes in animal PD models using an adeno-associated virus engineered to contain the glial fibrillary acid protein (GFAP) gene as a promoter in the experimental group. The adequacy of PD model establishment and improvement in parkinsonism were evaluated through a stepping test. The timelines of the experiments are summarized in Fig. 1. This study is reported in accordance with ARRIVE guidelines.

A53T α-synuclein overexpression model

To establish the animal PD model, the viral vector AAV_2-CMV-A53T-*SNCA*-EGFP, which overexpresses human mutant A53T α-synuclein, was used (Korea Institute of Science and Technology (KIST) virus facility (Seoul, South Korea); viral titer, 1.16 × 1013 GC/mL). The animals were sedated through an intraperitoneal injection of 35 mg/kg Zoletil and 5 mg/kg Rompun® and were secured in a stereotactic apparatus. A total of 2 µL of the AAV vector was injected unilaterally into the dorsal border of the right SNpc, with coordinates at anteroposterior (AP) − 5.4 mm, mediolateral (ML) + 2.0 mm relative to the bregma, and dorsoventral (DV) − 7.5 mm from the dura. The virus was infused at a rate of 0.3 µL per minute via a 33-gauge Hamilton syringe connected to an automated microinjection pump. Following the injection, the needle was retained in position for an additional 5 min to avoid any backflow of the solution.

NpHR transduction

The viral vectors AAV_{DJ}-GFAP-*NpHR*-mCherry (viral titer, 1.54×10^{13} GC/ml) was manufactured at the KIST virus facility (Seoul, South Korea), with the aim of selectively transducing NpHR in astrocytes. Two weeks after the injection of AAV_2-CMV-A53T-*SNCA*-EGFP, 2 µL of AAV_{DJ}-GFAP-*NpHR*-mCherry was stereotactically injected into the experimental group ($n = 8$) under general anesthesia via the same method described above with the same target. In the control group ($n = 8$), 2 µL of phosphate-buffered saline (PBS) was injected.

Optical fiber insertion and light stimulation

Two weeks following the NpHR transduction, all the animals were subjected to general anesthesia and secured in a stereotactic frame for the implantation. After making a scalp incision, four burr holes were carefully drilled for screw placement in the skull. The optical fiber (flat tip, 245 µm in diameter; Doric Lenses, Québec, QC, Canada) was inserted through a stereotactic cannula holder into the right SNpc, aligned with the coordinates used for the viral injection. It was then firmly affixed to the skull with screws using dental cement (Vertex, Zeist, The Netherlands). One week after fiber insertion, illumination was conducted on all animals using a 590 nm wavelength at a frequency of 50 Hz and a pulse duration of 10 ms for one hour, regulated by a pulse generator (Berkeley Nucleonics Corp., San Rafael, CA, USA). During the light exposure, the animals were allowed to move freely within glass cylinders (20 cm in diameter, 40 cm in height). The optical fiber was connected to a light source (Doric lenses) through a rotatory fiberoptic joint[37].

Stepping test

All animals underwent stepping tests one week prior to the viral injection of AAV_2-CMV-A53T-*SNCA*-EGFP, as well as 3 weeks and 5 weeks (immediately before and after illumination) following the procedure. The tests were conducted on a treadmill to a speed of 1.8 m every10 seconds. During the test, one forelimb was permitted to contact the moving treadmill, while the examiner restrained both hindlimbs and the opposite forelimb. Test were carried out for both the contralateral and ipsilateral forelimbs, and videos recordings were made to facilitate the counting of adjusted steps for one minute by the forelimb under observation. Each animals repeated the stepping test twice during each session, and the step counts from the two trials were averaged for analysis[37].

Tissue processing

Following the completion of the stepping test conducted one hour after the illumination, the animals were euthanized under general anesthesia through the intraperitoneal injection of Zoletil at a dosage of 35 mg/kg and Rompun® at 5 mg/kg. Subsequently, a transcardiac perfusion was performed using a solution of 0.9% saline mixed with 10,000 IU of heparin (Hanlim Pharm, Seoul, South Korea), and this was succeeded by a perfusion of 4% paraformaldehyde in PBS. After decapitating the animals, the optical fibers were carefully taken out, and the brains were extracted and subsequently fixed in 4% paraformaldehyde for 12 h. They were dehydrated in a 30% sucrose solution until they descended to the bottom. Using a microtome (Thermo Scientific), the brains were sectioned coronally at a thickness of 40 µm, ranging from AP -4.8 to -6.0 mm. The brain slices were then preserved in a free-floating manner in a solution of 0.08% sodium azide in PBS at 4 °C[37].

Immunohistochemical staining

Serial coronal sections of the SN underwent immunohistochemical staining for TH, GFAP, and GABA. Initially, the brain sections were rinsed in 0.5% bovine serum albumin (BSA; Bioworld) dissolved in PBS and then treated with a blocking solution (BSA, Triton X-100, sodium azide in PBS). Each section was then incubated overnight with specific primary antibodies: mouse anti-TH (1:2,000, Sigma), rabbit anti-GFAP (1:100, Sigma), and guinea pig anti-GABA (1:500, Sigma) in 0.5% BSA in PBS. Following this, the sections were treated with a secondary antibody (Alexa Fluor® 647 anti-mouse IgG (1:1,000; Invitrogen)) for 2 h. The labeled tissues were subsequently mounted using a fluorescent mounting medium (DAKO, Glostrup, Denmark).

Imaging and Stereological assessment

Fluorescence imaging was carried out utilizing a confocal microscope (Carl Zeiss, Oberkochen, Germany) and ZEN software (Carl Zeiss), employing three excitation wavelengths: 633 nm for TH, GFAP, and GABA, 561 nm for NpHR, and 488 nm for α-Syn. Three coronal sections containing the SNpc were selected for quantitative analysis based on their immunohistochemical staining of TH, GFAP, and GABA. MetaMorph® software (BioVision Technologies, Pennsylvania, USA), which provides image analysis features with a semiautomated quantification method, was utilized to evaluate the level of pathological human α-Syn, alongside NpHR, TH, GFAP, and GABA expression, in both experimental and control groups. The area of the SNpc was delineated manually using MetaMorph®, and the numbers, total area (μm^2), and average area (μm^2) positive for α-Syn, NpHR, TH, GFAP, GABA were computed.

Statistical analysis

Statistical analyses were conducted utilizing Prism Software (GraphPad, La Jolla, CA, USA). To evaluate the variation in the temporal patterns of the stepping test, we utilized a two-way repeated-measures analysis of variance along with the Bonferroni correction. The Mann–Whitney U test was applied for comparing the image quantification results of α-Syn, NpHR, TH, GFAP, and GABA between the two groups, considering a significance threshold of $p < 0.05$.

Data availability

available when requested.

Received: 5 July 2025; Accepted: 27 November 2025
Published online: 12 December 2025

References

1. Polymeropoulos, M. H. et al. Mutation in the alpha-synuclein gene identified in families with parkinson's disease. *Science* **276**, 2045–2047. https://doi.org/10.1126/science.276.5321.2045 (1997).
2. Spillantini, M. G. et al. Alpha-synuclein in lewy bodies. *Nature* **388**, 839–840. https://doi.org/10.1038/42166 (1997).
3. Meissner, W. G. et al. Priorities in parkinson's disease research. *Nat. Rev. Drug Discov.* **10**, 377–393. https://doi.org/10.1038/nrd3430 (2011).
4. Goedert, M., Spillantini, M. G., Tredici, D., Braak, H. & K. & 100 years of lewy pathology. *Nat. Rev. Neurol.* **9**, 13–24. https://doi.org/10.1038/nrneurol.2012.242 (2013).
5. Dehay, B. et al. Targeting alpha-synuclein for treatment of parkinson's disease: mechanistic and therapeutic considerations. *Lancet Neurol.* **14**, 855–866. https://doi.org/10.1016/S1474-4422(15)00006-X (2015).
6. Venda, L. L., Cragg, S. J., Buchman, V. L. & Wade-Martins, R. alpha-Synuclein and dopamine at the crossroads of parkinson's disease. *Trends Neurosci.* **33**, 559–568 (2010).
7. Deep-Brain Stimulation for Parkinson's Disease Study. Deep-brain stimulation of the subthalamic nucleus or the Pars Interna of the globus pallidus in parkinson's disease. *N Engl. J. Med.* **345**, 956–963. https://doi.org/10.1056/NEJMoa000827 (2001).
8. Deuschl, G. et al. A randomized trial of deep-brain stimulation for parkinson's disease. *N Engl. J. Med.* **355**, 896–908. https://doi.org/10.1056/NEJMoa060281 (2006).
9. Benabid, A. L., Chabardes, S., Mitrofanis, J. & Pollak, P. Deep brain stimulation of the subthalamic nucleus for the treatment of parkinson's disease. *Lancet Neurol.* **8**, 67–81. https://doi.org/10.1016/S1474-4422(08)70291-6 (2009).
10. Fischer, D. L. et al. Subthalamic nucleus deep brain stimulation does not modify the functional deficits or axonopathy induced by nigrostriatal alpha-Synuclein overexpression. *Sci. Rep.* **7**, 16356. https://doi.org/10.1038/s41598-017-16690-x (2017).
11. Musacchio, T. et al. Subthalamic nucleus deep brain stimulation is neuroprotective in the A53T alpha-synuclein parkinson's disease rat model. *Ann. Neurol.* **81**, 825–836. https://doi.org/10.1002/ana.24947 (2017).
12. Hirsch, E. C. et al. The role of glial reaction and inflammation in parkinson's disease. *Ann. N Y Acad. Sci.* **991**, 214–228. https://doi.org/10.1111/j.1749-6632.2003.tb07478.x (2003).
13. L'Episcopo, F. et al. Reactive astrocytes and Wnt/beta-catenin signaling link nigrostriatal injury to repair in 1-methyl-4-phenyl-1,2,3,6-tetrahydropyridine model of parkinson's disease. *Neurobiol. Dis.* **41**, 508–527. https://doi.org/10.1016/j.nbd.2010.10.023 (2011).
14. Liddelow, S. A. & Barres, B. A. Reactive astrocytes: production, function, and therapeutic potential. *Immunity* **46**, 957–967. https://doi.org/10.1016/j.immuni.2017.06.006 (2017).
15. Joe, E. H. et al. Astrocytes, Microglia, and parkinson's disease. *Exp. Neurobiol.* **27**, 77–87. https://doi.org/10.5607/en.2018.27.2.77 (2018).
16. Heo, J. Y. et al. Aberrant tonic inhibition of dopaminergic neuronal activity causes motor symptoms in animal models of Parkinson's disease. *Curr. Biol.* **30**, 276–291 e279. https://doi.org/10.1016/j.cub.2019.11.079 (2020).
17. Nam, M. H., Sa, M., Ju, Y. H., Park, M. G. & Lee, C. J. Revisiting the Role of Astrocytic MAOB in Parkinson's Disease. *Int. J. Mol. Sci.* **23**, 856. https://doi.org/10.3390/ijms23084453 (2022).
18. Enger, R. & Heuser, K. Astrocytes as critical players of the fine balance between Inhibition and excitation in the brain: spreading depolarization as a mechanism to curb epileptic activity. *Front. Netw. Physiol.* **4**, 1360297. https://doi.org/10.3389/fnetp.2024.1360297 (2024).
19. Bordey, A., Lyons, S. A., Hablitz, J. J. & Sontheimer, H. Electrophysiological characteristics of reactive astrocytes in experimental cortical dysplasia. *J. Neurophysiol.* **85**, 1719–1731. https://doi.org/10.1152/jn.2001.85.4.1719 (2001).
20. Verkhratsky, A., Parpura, V., Vardjan, N. & Zorec, R. Physiology of astroglia. *Adv. Exp. Med. Biol.* **1175**, 45–91. https://doi.org/10.1007/978-981-13-9913-8_3 (2019).
21. Cheng, H. C., Ulane, C. M. & Burke, R. E. Clinical progression in Parkinson disease and the neurobiology of axons. *Ann. Neurol.* **67**, 715–725. https://doi.org/10.1002/ana.21995 (2010).
22. Sofroniew, M. V. & Vinters, H. V. Astrocytes: biology and pathology. *Acta Neuropathol.* **119**, 7–35. https://doi.org/10.1007/s00401-009-0619-8 (2010).
23. Allaman, I., Belanger, M. & Magistretti, P. J. Astrocyte-neuron metabolic relationships: for better and for worse. *Trends Neurosci.* **34**, 76–87. https://doi.org/10.1016/j.tins.2010.12.001 (2011).
24. Kam, T. I., Hinkle, J. T., Dawson, T. M. & Dawson, V. L. Microglia and astrocyte dysfunction in parkinson's disease. *Neurobiol. Dis.* **144**, 105028. https://doi.org/10.1016/j.nbd.2020.105028 (2020).
25. Untiet, V. Astrocytic chloride regulates brain function in health and disease. *Cell. Calcium.* **118**, 102855. https://doi.org/10.1016/j.ceca.2024.102855 (2024).

26. Lee, H. J. et al. Direct transfer of alpha-synuclein from neuron to astroglia causes inflammatory responses in synucleinopathies. *J. Biol. Chem.* **285**, 9262–9272. https://doi.org/10.1074/jbc.M109.081125 (2010).
27. Rostami, J. et al. Human astrocytes transfer aggregated Alpha-Synuclein via tunneling nanotubes. *J. Neurosci.* **37**, 11835–11853. https://doi.org/10.1523/JNEUROSCI.0983-17.2017 (2017).
28. Ozoran, H. & Srinivasan, R. Astrocytes and Alpha-Synuclein: friend or foe? *J. Parkinsons Dis.* **13**, 1289–1301. https://doi.org/10.3233/JPD-230284 (2023).
29. Bennett, M. C. et al. Degradation of alpha-synuclein by proteasome. *J. Biol. Chem.* **274**, 33855–33858. https://doi.org/10.1074/jbc.274.48.33855 (1999).
30. Cuervo, A. M., Stefanis, L., Fredenburg, R., Lansbury, P. T. & Sulzer, D. Impaired degradation of mutant alpha-synuclein by chaperone-mediated autophagy. *Science* **305**, 1292–1295. https://doi.org/10.1126/science.1101738 (2004).
31. Chu, Y., Dodiya, H., Aebischer, P., Olanow, C. W. & Kordower, J. H. Alterations in lysosomal and proteasomal markers in parkinson's disease: relationship to alpha-synuclein inclusions. *Neurobiol. Dis.* **35**, 385–398. https://doi.org/10.1016/j.nbd.2009.05.023 (2009).
32. Dehay, B. et al. Pathogenic lysosomal depletion in parkinson's disease. *J. Neurosci.* **30**, 12535–12544. https://doi.org/10.1523/JNEUROSCI.1920-10.2010 (2010).
33. Lindstrom, V. et al. Extensive uptake of alpha-synuclein oligomers in astrocytes results in sustained intracellular deposits and mitochondrial damage. *Mol. Cell. Neurosci.* **82**, 143–156. https://doi.org/10.1016/j.mcn.2017.04.009 (2017).
34. Boyden, E. S., Zhang, F., Bamberg, E., Nagel, G. & Deisseroth, K. Millisecond-timescale, genetically targeted optical control of neural activity. *Nat. Neurosci.* **8**, 1263–1268. https://doi.org/10.1038/nn1525 (2005).
35. Park, S. et al. Optogenetic control of nerve growth. *Sci. Rep.* **5**, 9669. https://doi.org/10.1038/srep09669 (2015).
36. Bang, J., Kim, H. Y. & Lee, H. Optogenetic and chemogenetic approaches for studying astrocytes and gliotransmitters. *Exp. Neurobiol.* **25**, 205–221. https://doi.org/10.5607/en.2016.25.5.205 (2016).
37. Lee, E. J., Yoon, H. H., Park, E. S., Min, J. & Jeon, S. R. A novel animal model of parkinson's disease using optogenetics: representation of various disease stages by modulating the illumination parameter. *Stereotact. Funct. Neurosurg.* **96**, 22–32. https://doi.org/10.1159/000486644 (2018).
38. Lee, S. et al. Channel-mediated tonic GABA release from glia. *Science* **330**, 790–796. https://doi.org/10.1126/science.1184334 (2010).
39. Ishibashi, M., Egawa, K. & Fukuda, A. Diverse actions of astrocytes in GABAergic signaling. *Int. J. Mol. Sci.* **20**, 475. https://doi.org/10.3390/ijms20122964 (2019).
40. Akwa, Y. et al. Synaptic activity protects against AD and FTD-like pathology via autophagic-lysosomal degradation. *Mol. Psychiatry*. **23**, 1530–1540. https://doi.org/10.1038/mp.2017.142 (2018).
41. Astaburuaga, R., Quintanar Haro, O. D., Stauber, T. & Relogio, A. A mathematical model of lysosomal ion homeostasis points to differential effects of Cl(-) transport in Ca(2+) dynamics. *Cells* **8**, 96. https://doi.org/10.3390/cells8101263 (2019).
42. Chakraborty, K., Leung, K. & Krishnan, Y. High lumenal chloride in the lysosome is critical for lysosome function. *Elife* **6**, 785. https://doi.org/10.7554/eLife.28862 (2017).
43. Feng, X., Liu, S. & Xu, H. Not just protons: chloride also activates lysosomal acidic hydrolases. *J. Cell. Biol.* **222**, 236. https://doi.org/10.1083/jcb.202305007 (2023).
44. Hosogi, S., Kusuzaki, K., Inui, T., Wang, X. & Marunaka, Y. Cytosolic chloride ion is a key factor in lysosomal acidification and function of autophagy in human gastric cancer cell. *J. Cell. Mol. Med.* **18**, 1124–1133. https://doi.org/10.1111/jcmm.12257 (2014).
45. Lewis, S. A., Balcarek, J. M., Krek, V., Shelanski, M. & Cowan, N. J. Sequence of a cDNA clone encoding mouse glial fibrillary acidic protein: structural conservation of intermediate filaments. *Proc. Natl. Acad. Sci. U S A.* **81**, 2743–2746. https://doi.org/10.1073/pnas.81.9.2743 (1984).
46. Liddelow, S. A. et al. Neurotoxic reactive astrocytes are induced by activated microglia. *Nature* **541**, 481–487. https://doi.org/10.1038/nature21029 (2017).
47. Gao, Q., Li, Y. & Chopp, M. Bone marrow stromal cells increase astrocyte survival via upregulation of phosphoinositide 3-kinase/threonine protein kinase and mitogen-activated protein kinase kinase/extracellular signal-regulated kinase pathways and stimulate astrocyte trophic factor gene expression after anaerobic insult. *Neuroscience* **136**, 123–134. https://doi.org/10.1016/j.neuroscience.2005.06.091 (2005).
48. Zador, Z., Stiver, S., Wang, V. & Manley, G. T. Role of aquaporin-4 in cerebral edema and stroke. *Handb. Exp. Pharmacol.* **2009**, 159–170. https://doi.org/10.1007/978-3-540-79885-9_7 (2009).
49. Hayakawa, K., Pham, L. D., Arai, K. & Lo, E. H. Reactive astrocytes promote adhesive interactions between brain endothelium and endothelial progenitor cells via HMGB1 and beta-2 integrin signaling. *Stem Cell. Res.* **12**, 531–538. https://doi.org/10.1016/j.scr.2013.12.008 (2014).

Author contributions

Eun Jung Lee: ** Conceptualization, Data curation, Formal analysis, Investigation, Methodology, Validation, Visualization, Writing – original draft, Writing – Review & editing, **Hyung Ho Yoon: ** Date curation, Investigation, Validation, Writing – Review & editing, **Sang Ryong Jeon : Funding acquisition, Project administration, Resources, Supervision, Writing – Review & editing.

Funding

This study was supported by a grant (2024IL0018) from the Asan Institute for Life Sciences, Asan Medical Center, Seoul, Korea, and by the Korean Fund for Regenerative Medicine (KFRM) grant funded by the Korea government (the Ministry of Science and ICT, the Ministry of Health & Welfare) (23C0120L1).

Competing interests

The authors declare no competing interests.

Additional information

Correspondence and requests for materials should be addressed to S.R.J.

Reprints and permissions information is available at www.nature.com/reprints.

Publisher's note Springer Nature remains neutral with regard to jurisdictional claims in published maps and institutional affiliations.